

We are IntechOpen, the world's leading publisher of Open Access books Built by scientists, for scientists

6,600

Open access books available

178,000

International authors and editors

195M

Downloads

Our authors are among the

154

Countries delivered to

TOP 1%

most cited scientists

12.2%

Contributors from top 500 universities



WEB OF SCIENCE™

Selection of our books indexed in the Book Citation Index
in Web of Science™ Core Collection (BKCI)

Interested in publishing with us?
Contact book.department@intechopen.com

Numbers displayed above are based on latest data collected.
For more information visit www.intechopen.com



Chapter

Purification of Rainwater Using a Photocatalysis Technique to be Applied to Communities in Ciudad del Carmen, Campeche, Mexico

Carlos Montalvo, Claudia A. Aguilar, Rosa A. Martínez, Rosa M. Cerón, Alejandro Ruiz, Eric Houbbron and Juan C. Robles

Abstract

Small communities far from the municipal seat do not have access to drinking water, so many children suffer from various gastrointestinal diseases, which cause these children to grow up with nutritional deficiencies. In the state of Campeche, there are 300 sunny days. This energy can be used to install water treatment systems to make it drinkable. Therefore, a treatment system with heterogeneous photocatalysis was proposed using a zinc oxide catalyst doped with silver nanoparticles. The reactor has a metal structure with a flat plate where clay plates support the catalyst. Samples were taken every 2 h to carry out the corresponding analyses and in a period of 8 h of reaction. For the characterization of rainwater adhered to Mexican regulations. The results showed that there was 6400 NMP/100 mL for fecal coliforms at the beginning, and after 4 h, this parameter goes to <2 NMP/100 mL. Initially, the same happened for fecal coliforms; 9200 NMP/100 mL was determined. After 4 h, this parameter drops to <2 NMP/100 mL. The same behavior was observed with chlorides, hardness, and total alkalinity, which showed a tendency to decrease significantly. This confirms that the system works properly to eliminate organic compounds and purify rainwater.

Keywords: rainwater, zinc oxide, photocatalysis, drinking water, falling film photocatalytic reactor (FFPR)

1. Introduction

Water is one of the essential natural resources and, together with air, land, and energy, constitutes the four essential resources on which development is based [1].

Water, as a natural resource, is manipulated by man, thus altering its cycle. Water is extracted from ecosystems for use. But a greater supply of water to the cities brings with it a greater discharge of wastewater, which damages the vegetation and the quality of the subsequent discharge. It is here where the importance of sustainable

development must be recorded, which is the one that makes it possible to make the use of resources compatible with the conservation of ecosystems.

The amount of water we have on Earth is neither increasing nor decreasing, but the human population has grown drastically, and therefore, our need for this resource has also grown. Also, while the amount of water is constant, the way it is distributed over time is not: it is irregular throughout the year. It varies differently depending on global climatic conditions. In the same way, the diverse ecosystems, such as humid forests, pine forests, scrublands, grasslands, or deserts, influence the way and the amount of water that enters the aquifer systems, its conservation in the soil, or its passage into the atmosphere, which causes the availability of this resource to be variable in each region of the planet [2].

Access to good quality water is directly linked to human health and development. At present, the use of water for human consumption is limited since various sources contaminate most of the available fresh water.

In many parts of the world with high or medium rainfall, the quantity and quality of water necessary for human consumption is unavailable. Rainwater is used as a source of supply.

The observation of this acute and critical problem induced to seek and promote some practical methods that provide the small communities of the Municipality of Carmen, Campeche, with water of a certain quality for their consumption; therefore, in this investigation, the design and construction of a falling film photocatalytic reactor, in which a ZnO-Ag photocatalyst is fixed utilizing clay plates, with the purpose of degrading organic components through the incidence of solar radiation, is proposed.

The methodology considers the design, dimensions, and materials for constructing the photocatalytic reactor: the processes for preparing the solutions to be treated, the process of adequacy and photo deposition of the catalyst, and the optimal operating parameters of the falling film system.

2. Collection and storage

Rainwater harvesting and storage have been practiced for over 4000 years.

In the case of Mexico, the “aguadas” (artificial deposits) were used in pre-Columbian times to irrigate crops in small areas.

In archeological zones of the Yucatan peninsula, from the year 300 A.D., collection systems known as “chultus” were used, whose function is to collect rainwater from the patios and conduct it through channels to deposits built with stone to be utilized later [3]. The average annual rainfall for the Mexican territory is 1500 cubic kilometers of water. If 3% of this amount were used, it would be possible to supply 13 million Mexicans who currently do not have drinking water; two supplemental irrigations would be given to 18 million hectares of rainfed land; 50 million animals would be supplied, and 100,000 hectares of greenhouses would be irrigated [4, 5].

The collection, treatment, and use of rainwater is an essential source of water supply for human, livestock, and agricultural use and consumption for rural communities or populations of less than 2500 inhabitants, which have difficulties with their collection due to their topography, isolation, dispersion of hamlets, or lack of supply sources, whether surface or subway [4].

2.1 Water use in Campeche

In the state of Campeche, despite having several sources of fresh water and annual rainfall reaching an average of 1681.4 mm, there are no storage and treatment systems to use for human consumption, livestock, aquaculture, and vegetable irrigation, since there is no adequate technology to ensure that the water meets the specifications for these purposes [6].

The municipality of Carmen is located southwest of the state of Campeche, bordered to the north by the Gulf of Mexico and the city of Champotón, to the south by the state of Tabasco, to the east by the towns of Escárcega and Candelaria, and to the west by the municipality of Palizada. It is located between parallels 17°52' and 19°01' north latitude and meridians 90°29' and 92°28' west longitude of Greenwich. It has a territorial extension of 9720.09 km², representing 17.09% of the state's surface [4].

The municipality is in the Grijalva-Usumacinta hydrological region, the most crucial hydrological system in the state; due to its rainfall, periods of drought, and the topography of the terrain, it maintains a regime of irregular flows throughout the year, with the highest flows during the rainy season in summer and autumn, which decreases in winter and spring.

Today's world depends without exception on chemicals, whether to increase food production, protect health, or facilitate daily life [7, 8].

2.2 Water pollution

Three-quarters of the planet's surface is covered by water; approximately, there are 1385, 000, 000 km³ of water, of which 97.3% is salt water, 2.08% is frozen at the poles, and only 0.62% is available for the development and sustainment of human life [9].

Water pollution is defined as the presence of foreign substances or organisms in a body of water in such quantities and with such characteristics that they prevent its use for specific purposes [4]. Such contamination can be of natural or anthropogenic origin, a direct consequence of the development of water resources [4].

Such pollution can be of natural or anthropogenic origin, directly from sewage or industrial runoff (point sources) or indirectly from air pollution or agricultural or urban runoff (non-point sources) [10].

There is a great variety of components in water, which their nature or size can classify. Their physical or biological nature can distinguish them by size; they are classified as suspended matter, colloidal matter, and dissolved matter.

Chemical pollutants include organic and inorganic components, each with specific characteristics in contaminated water. The presence of organic compounds decreases the amount of oxygen dissolved due to their biodegradation by aerobic microorganisms. On the other hand, the presence of inorganic compounds is related to toxicity, especially in the case of heavy metals. Some inorganic compounds, such as sulfites and nitrites, oxidize, generating a demand for dissolved oxygen [11, 12].

Physical pollutants include thermal pollution due to the discharge of slightly hot water used in heat exchangers, turbidity (caused by suspended solids), color, foaming, and radioactivity [11].

Biological contaminants include remains of plants, animals, and microorganisms. These contaminants are responsible for transmitting diseases, some of which are transmitted by biological pollutants, such as cholera, typhoid, paratyphoid, and so on.

2.3 Water decontamination

The use of water is limited by its quantity and quality. Water quality used to be qualified only by some physical parameters such as appearance, color, taste, and odor, and now, with the scientific and technological advances that have had an impact on the development of analytical techniques and processes capable of identifying a wide range of compounds, giving way to chemical and biological parameters, to such an extent that it is possible to make drinking water by purifying wastewater.

Physical parameters are the characteristics that the senses can perceive, such as suspended solids, turbidity, color, taste, odor, and temperature.

In water, there are biological species of different sizes and complexity for which there are biological parameters; the presence of specific organisms, bacteria, viruses, and protozoa, can be used as an indicator of a contaminant.

2.4 Heterogeneous photocatalysis

Heterogeneous photocatalysis is a discipline whose main objective is to decrease the energy activation of a photochemical reaction. Heterogeneous photocatalysis includes various reactions: moderate or total oxidation, dehydrogenation, metal deposition, water detoxification, removal of gaseous pollutants, and so on. It can be considered one of the new “advanced oxidation technologies” for water and air purification treatments [13].

Photocatalysis differs from conventional heterogeneous catalysis by activating the solid catalyst through photo absorption instead of thermal activation [13, 14].

This type of activation requires a semiconductor material as a catalyst, which must be provided with radiation energy higher than its forbidden band.

The overall process is like a conventional catalysis, which can be broken down into five independent steps:

1. Transfer of reactants from the fluid phase to the surface
2. Adsorption of at least one of the reactants
3. Reaction of the adsorbed phase
4. Desorption of the products
5. Removal of the products from the interface region

Three components are fundamental for a heterogeneous photocatalytic reaction: a photon source (with appropriate wavelength), a catalytic surface (usually a semiconductor material), and an electron acceptor, which in many cases is oxygen.

Charge carriers are transferred to the photocatalytic surface, allowing REDOX reactions with the adsorbed reactants. On the catalytic surface, REDOX reactions are separated into oxidation and reduction processes, involving, on the one hand, conduction band electrons and electron acceptors, for example, oxygen molecules ($e_{CB}^- + A \rightarrow A^{\bullet-}$), and, on the other hand, valence band holes and adsorbed electron donors, such as organic molecules or generally specific pollutants ($h_{VB}^+ + D \rightarrow D^{\bullet+}$). Indirect oxidation reactions also occur by forming the highly oxidizing hydroxyl radical (HO•) generated by water oxidation by the voids [15–17].

Each ion formed then reacts to form an intermediate and end product. Because of the reaction, photonic excitation of the catalyst appears as the initial step of the entire catalytic system. Hence, the photon efficiency must be considered a reactant, and the photon flows as a special fluid, the “electromagnetic” phase. The photon energy is adapted to the adsorption of the catalyst, not to that of the reactants. The activation of the process goes through the excitation of the solid but not through the reactants. As demonstrated below, the adsorbed phase has no photochemical process, only a proper heterogeneous catalysis regime [13].

Whenever different semiconducting materials have been tested under comparable conditions for the degradation of the same compounds, TiO₂ has generally been shown to be the most active. This semiconductor is of particular interest as it can utilize natural (solar) UV because it has an appropriate energy separation between its valence and conduction bands, which can be overcome by the energy content of a solar photon (390 nm > γ > 300 nm) [18, 19].

Systems based on disinfection by heterogeneous photocatalysis using solar radiation have several advantages, such as [19–22]:

Non-consumption of high-value oxidizing agents and high production of TiO₂.

Since the ultraviolet radiation necessary for catalyst activation can be obtained from solar radiation, this system consumes minimal maintenance energy and no external energy consumption during operation.

The oxidants produced are high-powered and non-discriminating, with the advantage of eliminating most microorganisms and degrading or mineralizing most organic pollutants.

It can be applied in rural areas or areas of difficult access since other similar technologies, such as UV irradiation or ozone application, require an external energy source.

2.5 Catalysts

Zinc oxide (ZnO) is an economically accessible metal oxide, easily detectable. Low energy light can excite it, absorbing part of the solar radiation incident on the earth's surface. It has received interest in removing and destroying recalcitrant organic compounds within the photocatalysis technology [23, 24].

ZnO exhibits a broad spectrum of biocidal activity toward different bacteria, fungi, and viruses given to the production of reactive oxygen species and the release of Zinc ions (Zn²⁺); it is also demonstrated that the synthesis of this metal oxide by green chemistry routes has a higher bioactivity, which is possibly attributed to the greater surface area, higher absorption capacity, crystallinity, and transmission [24–26].

Ag (Silver) is the most studied agent, and therefore, more information is available regarding its mechanism of antimicrobial activity; it is active against Gram-negative (*Escherichia coli*) and Gram-positive (*Staphylococcus aureus*) bacteria [26].

3. Methodology

3.1 Reagents

The reagents used throughout the different processes for the development of the research work in the treatment of rainwater disinfection are:

Zinc oxide of the J. T. Baker brand, silver sulfate of the Fermon brand, pyridine of the Aldrich brand, silver nitrate of the J.T. Baker brand, sodium chloride of Baker, sodium chloride of the Zeus brand, potassium chromate of the Fermon brand, ammonium chloride of the Baker brand, and ammonium hydroxide of the Baker brand, among others, especially in the analysis of rainwater samples.

3.2 Equipment

During the realization of this project, equipment located in the Catalysis Laboratory of the Faculty of Chemistry UNACAR was used, as described in the following **Table 1**:

3.3 Falling film photocatalytic reactor (FFPR)

The falling film photocatalytic reactor (FFPR) is designed with a metallic structure base that provides a surface area of 1.00 m²; with the impregnated catalyst, the contact area is increased to 852 m², with a height of 80 cm; the photoreactor presents an inclination that can be positioned at an angle of 15, 30, and 45°; the feeding works with a recirculation system by gravity and pressure action making use of a centrifugal electric pump with magnetic dragging that is supported by distributed hoses the water through channels that at the beginning circulate the water on the surface of the photoreactor and at the end lead the water to a tank where the experimental water is kept in a container, thus completing the connection of the recirculation system; the water flow is controlled with a ball valve as shown in **Figure 1**.

The materials used for the construction of this reactor are listed in **Table 2**. It is made up of a metallic structure, a ceramic bed where the doped catalyst is found, and a pumping system.

3.3.1 Catalyst support

Red clay plates support the catalyst on a porous surface due to their adsorption capacity, stability, and non-toxicity. To cover the area of 1.00 m², ten plates are selected, and the minimum necessary cuts are made to fit the reactor. They are leveled with sandpaper on one side to homogenize the surface and washed to eliminate loose dust. Finally, they are placed in the muffle for 1 hour at 550°C to eradicate moisture and organic matter.

Nombre	
Analytical balance	Brand: VELAB, Model: VE-204
Mufla	Brand: Fisher Scientific, Model: 550-14
UV-vis spectrophotometer	Brand: Agilent Technologies, Model: CARY – 60
Multiparameter meter	Brand: Hach Co, Model: HQ40d
Gas extraction hood	Brand: Formacero, Model: 120 Serie 2
Centrifugal electric pump	Brand: Laing Thermotech, Model: LMB0510196
Electric stove	Brand: Aceq Lab. Model: HRN-1003 de 110 Lts
Vacuum pump	Brand: Rocker Lab, Model: Rocker 300

Table 1.
Equipment used.

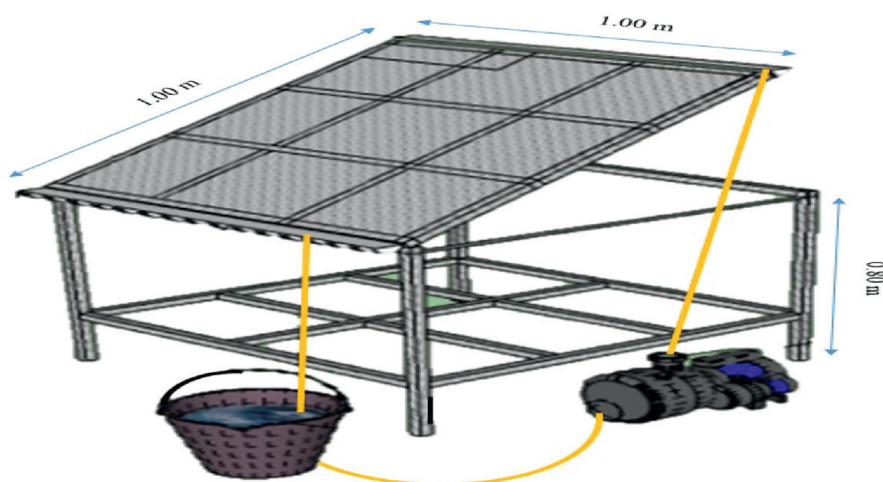


Figure 1.
 Schematic diagram of the FFPR.

Quantity	Material
10 units	Red clay plates of 30 × 30 × 2.5 cm
1 m ²	Galvanized stainless steel mirror finish caliber sheet 28
23 mL	Tubular profile de 1 × 1”
4 mL	Screed angle de 90° × 1 × 1/8 “
1 mL	Carbon steel pipe 2.”
1 unit	Carbon steel coupling 1”
3 units	Butt hinge of 1”
1 unit	Electro centrifugal pump 1/2 Hp
3 m	water hose 1/2”
1 unit	ball valve for the water of 1/2”
6 units	UV lamps 365 nm 15 w

Table 2.
 List of materials for the construction of the RFPD.

3.3.2 Catalyst synthesis

To carry out the dry impregnation synthesis of the catalyst, a solution of distilled water and zinc oxide at non-fixed concentrations is prepared, preparing a total of 33 g of ZnO for 1600 mL of distilled water, after which it is applied on the surface face of each clay plate to cover the entire reactor and is left to stand for 90 minutes. After this step, to dry, adhere, and activate the catalyst, the plates are introduced into the muffle for 2 hours at 550°C.

3.3.3 Catalyst doping

Once the catalyst is supported on the plates, the catalyst is doped with silver nanoparticles, starting with the preparation of a solution of distilled water and avocado sulfate at a concentration of 400 ppm for 8 liters of distilled water, which is carried out with the photo deposition method on the impregnated catalyst, and the

recirculation of the silver sulfate solution is started. At the same time, it is irradiated with six ultraviolet light lamps of 365 nm and 15 watts of power for a time of 6 hours and is left to stand for 2 hours; the next step is activation by calcination, and for this, each plate is introduced to the muffle for 2 hours at 550°C. Ultimately, the plates are placed on the reactor, ready to test its functionality and disinfect the rainwater.

3.3.4 Reactor start-up testing

Four water absorption tests were performed before using the FFPR to treat rainwater. The results of this absorption are shown in **Table 3**.

It was shown that before incorporating the solution to be treated over the reactor, it was necessary to include at least 3 L of water and consider that the clay tiles absorb this amount.

To ensure reliability in the reaction system, initial tests are made with the degradation of the pyridine compound based on previous research results [27]. Initial concentrations of 50 parts per million (ppm) of the pyridine compounds were used as the model compound, which was treated for 8 h, taking samples of 50 mL every 2 hours, which were analyzed in a Cary-60 Uv-vis spectrophotometer. In this equipment, a sweep was performed from 200 to 600 nm.

3.4 Rainwater samples

Collecting, preserving, and storing samples for subsequent characterization and microbiological decontamination are necessary for the disinfection treatment of rainwater over the photocatalytic reactor.

The collection of 25 samples of 200 mL of rainwater was carried out during the rainy season in a period from June to September in Ciudad del Carmen, Campeche, at location 18.642522, -91.816223, with a collection system built to capture water directly from the source, in the open air; they were preserved and stored under refrigeration until they were handled for the corresponding characterization.

3.5 Characterization of rainwater

The physical and chemical analyses are carried out by the Mexican Official Standard NOM-127-SSA1-1994, "Environmental Health, water for human use and consumption-permissible quality limits and treatments to which water must be subjected for its potabilization." In this case, 20 L of rainwater was treated in batches and treated in the reactor for 8 hours with exposure to sunlight; samples were taken every hour to see the progress of the disinfection or treatment given to this water.

Test number	Incorporated water (L)	Exposure time (h)	Water absorbed (L)
1	10	8	4
2	10	8	3.5
3	20	8	3
4	20	8	3

Table 3.
Analysis of absorption tests.

In the Teaching, Research and Services, Management and Environmental Control Laboratory of the Faculty of Chemical Sciences of the Veracruzana University Orizaba campus, Veracruz., samples were analyzed, according to the official Mexican regulations.

Table 4 shows the parameters analyzed and the regulations applied; each parameter is analyzed utilizing an official Mexican standard.

4. Results of the project

The results obtained throughout this project of constructing a photocatalytic reaction system to treat rainwater and be used in small communities of Carmen, Campeche, are shown.

The construction of the photocatalytic reaction system in its different stages of development and the tests for using the reactor are shown. And in the same way, results regarding the collection, handling, and physical, chemical, and microbiological analyses of rainwater samples are presented.

4.1 Construction of the falling film photocatalytic reactor

For the construction of the falling film photocatalytic reactor, as the design was presented in the methodology, the materials listed in **Table 2** were used.

As shown in **Figure 2**, its metallic structure provided an occupation area of 1 m² to support the clay plates that, at the same time, kept the catalyst for its subsequent impregnation and doping process, working at an angle of 30° inclination (**Figure 2a**).

Test carried out	Mexican regulations
Physical Characterization	
Temperature	NMX-AA-007-SCFI-2013 [28]
Hydrogen Potential	NMX-AA-008-SCFI-2016 [29]
Total Solids	NMX-AA-034-SCFI-2001 [30]
Volatile Total Solids	NMX-AA-034-SCFI-2001 [30]
Total Suspended Solids	NMX-AA-034-SCFI-2001 [30]
Volatile Suspended Solids	NMX-AA-034-SCFI-2001 [30]
Total Dissolved Salts	NMX-AA-034-SCFI-2001 [30]
Chemical Characterization	
Total Chlorides	NMX-AA-073-SCFI-2001 [31]
Total hardness	NMX-AA-072-SCFI-2001 [32]
Total Acidity and Alkalinity	NMX-AA-036-SCFI-2001 [33]
Chemical Oxygen Demand	NMX-AA-030-SCFI-2001 [34]
Microbiological analysis	
Determination of fecal and total coliforms	NMX-AA-042-SCFI-2015 [35]

Table 4.
 Tests are carried out according to the corresponding regulations.

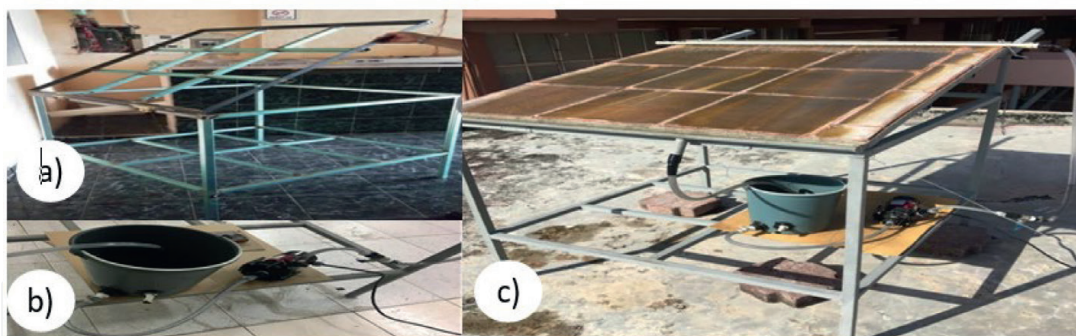


Figure 2. Construction stages of the FFPR. (a) Metallic structure, (b) recirculation system, and (c) FFPR operating in previous degradation tests.

We also proceeded to incorporate the recirculation system (**Figure 2b**), which was supported by the electric pump to supply the liquid through hoses that lead it to the distribution channel, descending through the surface of the reactor to be collected directly in the collection channel that leads the liquid to an outlet with a hose so that the liquid reaches the collection tank again.

4.2 Catalyst support

For the catalyst support, clay plates were used that were subjected to a selection process during the process (**Figure 3a**). In addition, they were adapted to the reactor to support the total area (**Figure 3a**); and finally, they were subjected to a calcination process (**Figure 3b**).

4.3 Catalyst impregnation

For the impregnation of the support, the solution prepared with the ZnO catalyst and distilled water was used (**Figure 4a**); later it was dried to remove the liquid trapped in the pores (**Figure 4b**) then it's calcined at 550 °C for 1 h, and the activation was achieved of the catalyst. Calcination increases the surface concentration and generates a catalyst with uniform distribution (**Figure 4c and d**).



Figure 3. (a) Catalyst support and placing clay plates on the FFPR, (b) calcination process, observing the porosity and homogeneity on the surface of the plate.

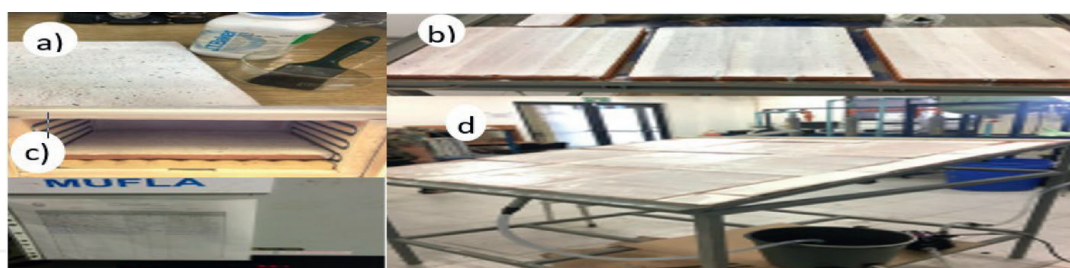


Figure 4. ZnO catalyst impregnation process (a) and (b); impregnated support plates and fixation of the support on the FFPR and calcination of a plate in muffle at 550°C (c), completing the impregnation with the catalyst on the FFPR (d).

4.4 Catalyst doping

For the doping of the catalyst with Ag^+ nanoparticles, the solution prepared with Ag_2SO_4 and distilled water (**Figure 5a**) was used to initiate recirculation under exposure to UV light (**Figure 5b**) and thus achieve the photo deposition of the silver (**Figure 5c**). Finally, it was calcined to reach the activation of the bactericidal metal.

4.5 RFPD tests

The falling film photocatalytic reactor demonstrated its feasibility in the photo-degradation of the organic pyridine compound in an initial concentration of 50 ppm using a ZnO – Ag^+ -doped catalyst.

Figure 6 shows the monitoring of the photodegradation of the organic compound utilizing absorbance graphs at a wavelength of 200 to 600 nm. However, more excellent activity of the compound was observed in a range of 200 to 300 nm.

The organic compound presented a characteristic maximum peak of the same at a wavelength of 256 nm and simultaneously showed distinct intermediate peaks of the pyridine [36].

The pyridine photodegradation test was carried out with the same initial concentration for 6 h, taking a sample every 2 h to observe its behavior.

In the degradation of the pyridine, as shown in **Figure 7**, it can be observed how the behavior of the pyridine changes for the reaction time.

It is observed that in the time of zero hours ($t = 0$ h), the natural behavior of the compound is shown, which ensures that the organic compound is present in the solution, having an initial concentration of 50 ppm and showing absorbance of 2351

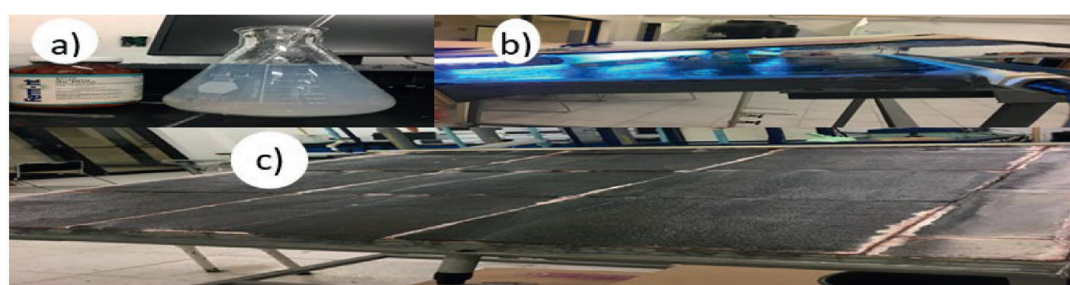


Figure 5. Catalyst doping process with Ag^+ nanoparticles. (a) Preparation of the solution with silver sulfate, (b) doping process by photo deposition on the support impregnated with the catalyst; (c) support of the FFPR finishing the photo deposition.

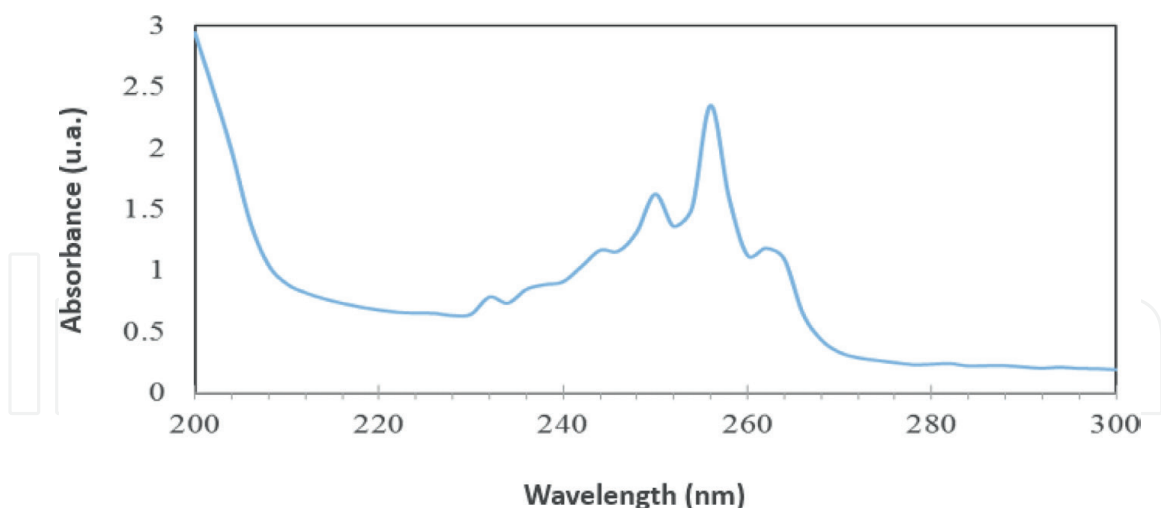


Figure 6.
A spectrum of organic compound pyridine with a concentration of 50 ppm.

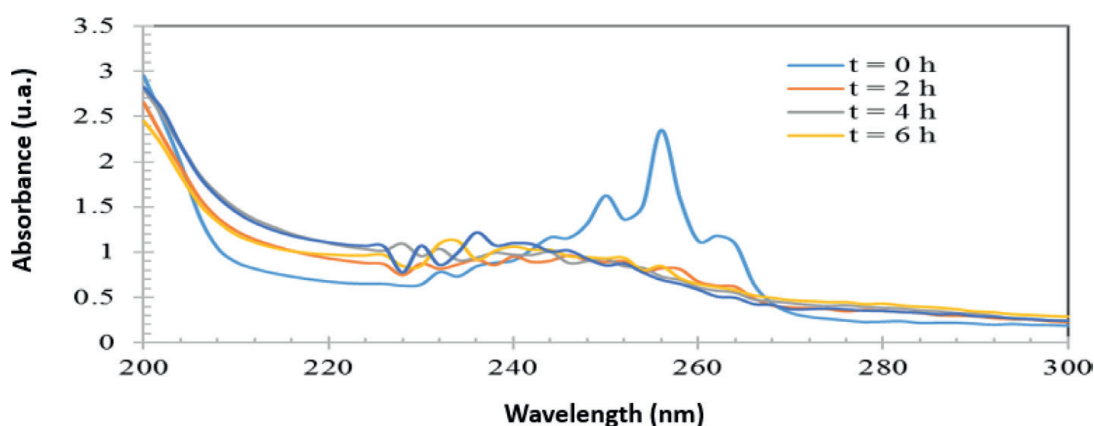


Figure 7.
The organic compound pyridine was degraded on the falling film photocatalytic reactor in the presence of the ZnO – Ag⁺-doped catalyst for 6 h.

arbitrary units (u.a.); then, in the elapsed time of 2 hours ($t = 2$ h) of the degradation on the photoreactor, it can be observed that the concentration drops to 0.825 u.a., presenting a degradation of 65%; for the 4 hours of reaction ($t = 4$ h), it shows a decrease in the concentration to 0.731 u.a. resulting in a 69% degradation; later, after 6 hours of reaction ($t = 6$ h), it presents a slight increase in concentration to 0.845 u.a.; however, after 8 hours of reaction ($t = 8$ h) in the system, it is possible to drop to 0.695 u.a., reaching a final degradation of 70% [22].

It should be noted that randomly generated peaks appear from the tempo of 2 h to the time of 8 h because the main compound is degrading. Still, alternately, there is the presence of other intermediate compounds being formed.

Figure 8 shows the spectrophotometer reading carried out in a degradation of the same compound at initial concentrations of 50 ppm. In this image, you can better appreciate the formation of intermediate compounds after the first 2 h of photodegradation; such shapes can be attributed to the presence of 2 hydroxy pyridines, as reported by Montalvo (2009) [36]; however, at 4 h, the pyridine peak disappears.

In **Figure 9**, the trend line shows a reliability of 95.5% concerning the average data represented that oscillate in the initial concentration from 50 ppm to 16.22 ppm,

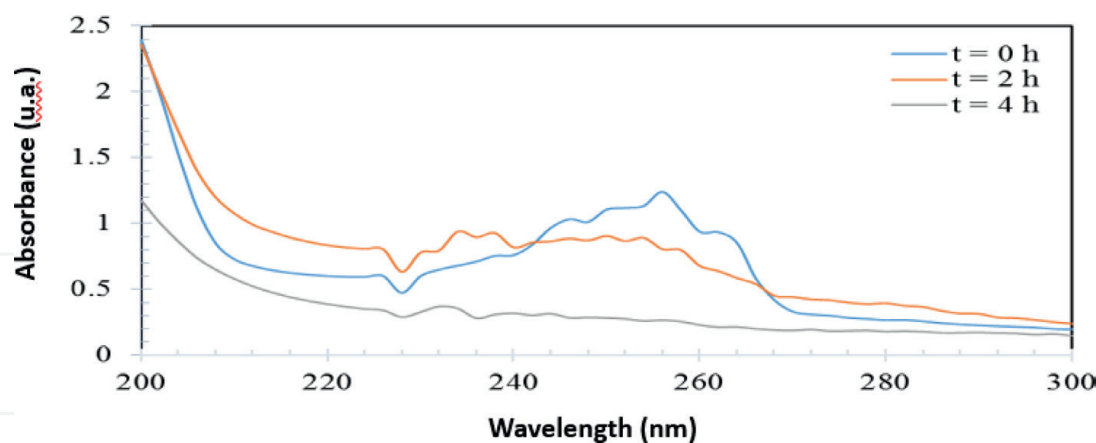


Figure 8.
Degradation of the organic compound pyridine during a period of 4 h.

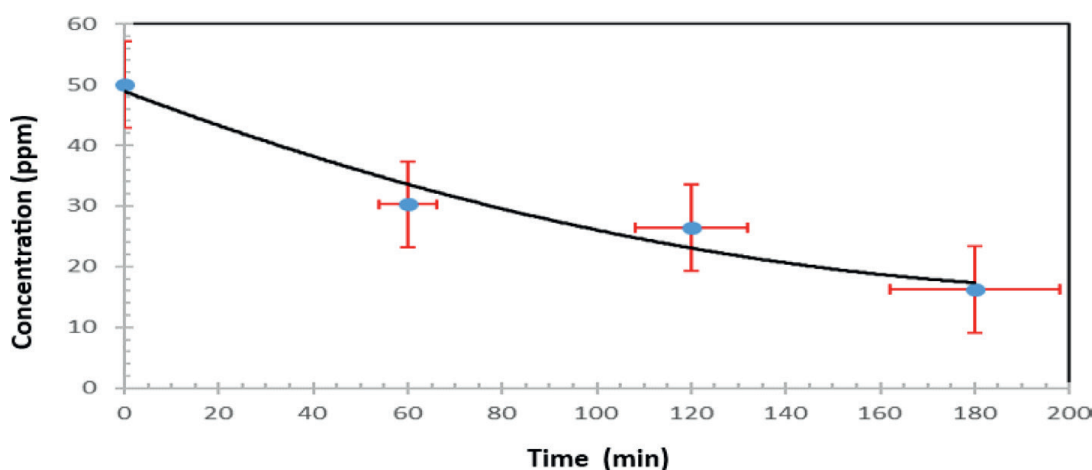


Figure 9.
Line of tendency and standard deviation of the degradation of the organic compound PYR in a period of 3 h.

considering a time of 0 to 180 minutes, which was the most representative time in the photodegradation tests.

Likewise, the standard deviation representing the variations of the average obtained in the data of the different photodegradation tests carried out to get these results is evidenced.

Figure 9 describes the degradation of the organic compound pyridine; it starts from a concentration of 50 ppm in its initial time. After 60 min of the photodegradation test, it degrades to 30.2599 ppm; after 120 min of degradation, the concentration of the compound drops to 26.3962; for a time of 180 min, the concentration is lowered to 16.2276 ppm.

In **Figure 10**, you can satisfactorily see the increase in the photodegradation of the organic compound; at time zero, there is no result since the presence of the contaminant is intact in the solution; for a time lapse of 60 min of photodegradation, there is a reduction from 50 ppm to 30.2599 ppm, achieving a percentage of photodegradation of 39% concerning the initial concentration of the original compound; it can also be observed that at 120 min, the photodegradation increases by 20% and after 180 minutes, a photodegradation of 68% [27].

Such results obtained are adequate due to the conditions managed, referring to the volume worked under direct exposure to sunlight.

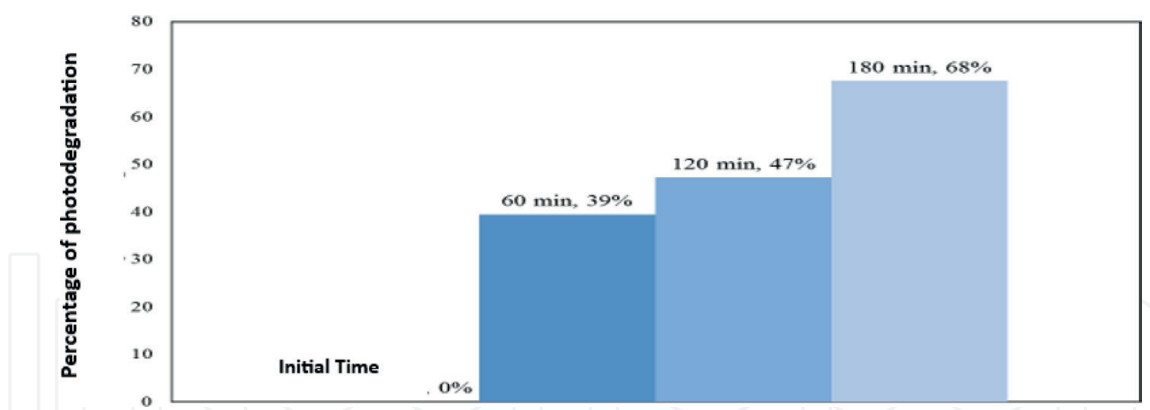


Figure 10.
Average percentage of degradation of the organic compound pyridine during 3 h.

4.6 Obtaining kinetic parameters

Various studies show that the first step in the photocatalytic degradation of organic compounds follows first-order or zero-order kinetics. The results clearly show that the reaction rate depends fundamentally on the concentration of the reaction (Figure 9), so it can be said that it follows first-order kinetics or is like first-order kinetics:

$$r_a = \frac{dC}{dt} = K \quad (1)$$

By integrating the velocity equation, the following function is obtained:

$$\ln \frac{C}{C_0} = -K_{\text{apparent}} t \quad (2)$$

Which is equivalent to $C_0 - K_{\text{apparent}} t$.

Figure 11 plots the logarithms of the normalized concentrations $\log(C/C_0)$ vs. reaction time. The values of the apparent reaction constant were obtained by linear regression.

The data are necessary to obtain the K_{apparent} kinetic constants from the line equation. **Figure 11** shows the photocatalytic degradation of pyridine, and this follows a pseudo-first-order reaction since the reaction rate is the same as the concentration increases. **Table 5** shows the values of this constant obtained as the same from **Figure 11**.

4.7 Sample collection

A collection system was built to capture rainwater directly from the source, in the open sky, and thus collect 25 samples that were preserved, stored, and refrigerated until their characterization and the final analysis (**Figure 12**). These samples were collected during the rainy season from June to September in the municipality of Carmen city, Campeche.

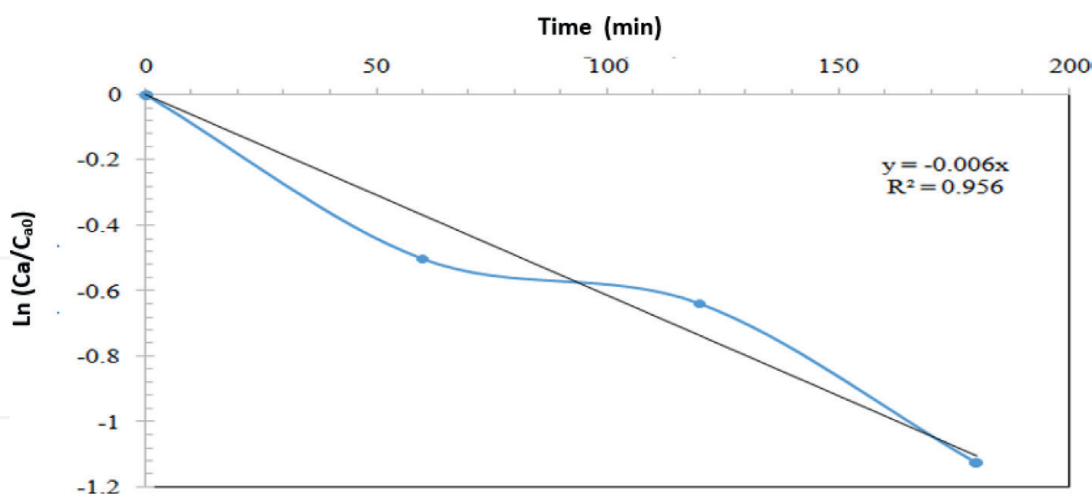


Figure 11.
 Kinetics of the pyridine reaction using $ZnO-Ag^+$ as a catalyst.

$C=C_0$ (ppm)	K_{apr} (min^{-1}) irradiated with sunlight	R^2	$r_0, (t = 0)$ (ppm/min)
50	0.006	0.956	0.3

Table 5.
 The apparent velocity (min^{-1}) for the degradation tests utilizing a $ZnO-Ag^+$ reactor.

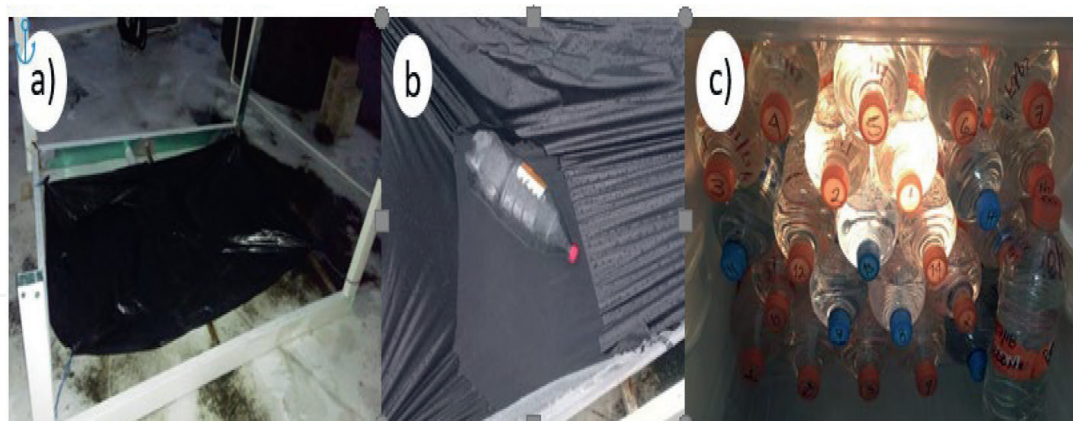


Figure 12.
 Sample collection. a) Construction of the rainwater collection system, b) water collected during seasonal rain, and c) samples stored and refrigerated.

4.8 Characterization and analysis of rainwater samples

The Official Mexican Standard NOM-127-SSA1-1994 [37], referring to Environmental Health regarding water for human use and consumption, establishes the permissible limits of quality and treatments to which water must be subjected for purification. For this reason, it is considered to carry out the pertinent characterization tests on the water samples, following the criteria it establishes.

The average results obtained from the tests carried out during the characterization and physical and chemical analyses obtained are shown in **Tables 6** and **7**, respectively, as well as their maximum permissible limit according to regulations.

Test carried out	Sample evaluated	Average value obtained	Maximum permissible limit	Unit of measurement
Temperature	01–18	26.2	40	°C
Total Solids	04, 05, 07, 12	28	200	mg/L de STT
Volatile Total Solids	04, 05, 07, 12	22	120	mg/L de STV
Total Suspended Solids	04, 05, 07, 12	8	100	mg/L de SST
Volatile Suspended Solids	04, 05, 07, 12	6	70	mg/L de SSV
Total Dissolved Salts	04, 05, 07, 12	20	1000	mg/L de SDT

Table 6.
Average results obtained from physical tests carried out on rainwater according to the corresponding regulations.

Test carried out	Sample evaluated	Average value obtained	Maximum permissible limit	Unit of measurement
Hydrogen Potential	01–18	7.33	6.5–8.5	Units of pH
Total Chlorides	10, 11, 18	0.0013	250.00	mg Cl ⁻ /L
Total hardness	01, 09, 14, 17	3.003	500	mg/L de CaCO ₃
Alkalinity	02,03,08,15,16	13.2	—	Units of pH
Total Acidity	02,03,08,15,16	2.4	—	Units of pH
Chemical Oxygen Demand	06, 13	0.0002	<1	mg/L COD

Table 7.
Average results obtained from chemical tests carried out on rainwater according to the corresponding regulations.

The analyzed parameters show average results below the maximum permissible limit since, as previously mentioned, the rainwater was collected directly from the source in the open sky without having contact with any contaminated surface and was later stored in refrigeration, to preserve its properties until reaching the corresponding characterization analysis.

4.9 The treatment of collected rainwater

When carrying out the photodegradation treatment of rainwater collected in a cistern, the 20-L sample was recirculated in the RFPD to maintain contact of liquid with the surface of the reactor with the supported and impregnated catalyst and under the effect of sunlight for eight hours, a 1 L sample was taken every 4 h to carry out the tests on the main parameters and verify the effectiveness of the system when degrading the organic components present. The data shown in **Table 8** were obtained from the tests carried.

The data shown in **Table 8** show that the rainwater that was not promptly used for domestic use began to be collected through the roof, conducted by pipes to be stored in a typical cistern, where, by not having an immediate disinfection treatment, it became rich in microbiological contaminants (bacteria, fungi, algae, etc.) by carrying garbage, organic matter from the environment, bird droppings or other animals that circulate on the roof, and therefore, stored water becomes a cause of concern for health care.

Each microorganism grows individually. However, ambient temperature and an average pH of 6.69 are critical factors that increase the growth rate of

Parameter/Time (h)	0	4	8	Unit	Official Mexican Standard
Hydrogen Potential	6.44	7.07	6.55	pH	NMX-AA-008-SCFI-2006 [29]
Total Dissolved Salts	452	423.5	196.5	mg/L	NMX-AA-034-SCFI-2015 [30]
Chlorides	18.85	26.4	30.4	mg/L	NMX-AA-073-SCFI-2001 [31]
Hardness	68.79	158.52	220.33	mg/L	NMX-AA-072-SCFI-2001 [32]
Total alkalinity	121.45	120	125	mg/L	NMX-AA-036-SCFI-2001 [33]
Total coliforms	92,000	<2	<2	NMP/100 mL	NMX-AA-042-SCFI-2015 [35]
Fecal coliforms	6400	<2	<2	NMP/100 mL	NMX-AA-042-SCFI-2015 [35]

Table 8.

Results obtained from the analysis of rainwater collected according to the corresponding regulations.

microorganisms, mainly mesophilic bacteria, total coliforms, fecal [thermotolerant] bacteria, and *Escherichia coli*.

Regarding the dissolved salts, it can be noted that there was a decrease from 452 to 196.5 mg/L, which favors the water quality, an indicator of the effectiveness of the photocatalytic process of the water disinfection treatment.

Chloride ions are one of the most widespread ions in natural waters. It is not usually an ion that poses portability problems to drinking water, although it is an indicator of water contamination due to human action. The maximum permissible chloride concentration for human consumption is 250 mg/L. Therefore, an average of 25.22 mg/L is an acceptable average value for using water stored in a cistern.

Magnesium and calcium salt depend fundamentally on the geological formations that the water traverses before its collection. In this case, the hardness increases from a value of 68.79 to 220.33 mg/L; it is considered hard water, which means that it contains more calcium and magnesium minerals; as the hardness of water increases, more calcium and magnesium are dissolved. Magnesium and calcium are positively charged ions. Due to their presence, other positively charged ions will dissolve less easily in hard water than in water that does not contain calcium and magnesium.

Considering the total alkalinity parameter with an average value of 122.15 mg/L, which is an acquired value of the materials added in domestic uses due to the cistern water storage system, showing the presence of hydroxides, carbonates, and bicarbonates of elements such as calcium, magnesium, sodium, potassium, or ammonia, considered as biological nutrients.

Total coliforms and fecal coliforms are the most significant indicators of microbiological contamination; the presence and degree of fecal contamination are essential factors in evaluating water quality [38, 39]. The initial tests (t = 0 h) present a significant NMP of total and fecal coliforms, 92,000 and 6400 NMP/100 mL, respectively. In both cases, the effectiveness of the photocatalytic reaction is verified in the tests carried out at t = 4 h, eliminating thoroughly any coliform present in the medium.

5. Conclusions

Given the nature of the construction of the falling film photocatalytic reactor, it is concluded that it satisfactorily fulfilled the function for which it was designed when testing its functionality in the previous tests and the same degradation of rainwater collected in the cistern. It is an alternative for the development of future research with different contaminants and at larger scales since it did not show any complication in the mineralization of organic compounds and microorganisms using zinc oxide catalyst doped with Ag⁺ nanoparticles, interacting under the incidence of sunlight.

The clay plates, due to their composition and their manufacturing, had deformations due to the preparation on the surface face and the cuts made to adapt the reactor to the size, creating pathways through which the water had greater ease in moving, and at the same time, crests were created where the passage of the flow of the treated liquid over the reactor occurred to a lesser extent.

However, for use as support, the clay was an excellent receptor of the catalyst since a uniform impregnation of ZnO on the clay was achieved, increasing the contact area of the catalyst from 1 m² of the surface area to 852.5 m².

The doping of the ZnO catalyst with the photo deposition of Ag⁺ nanoparticles is a proven good alternative for the photocatalytic degradation in the mineralization of contaminating microorganisms, showing the breakdown of their cell wall in a period of 4 hours. At the same time, the degradation of the organic compound “pyridine” is verified, showing degradation efficiency of up to 68% in a time of 3 h.

The operating parameters of the falling film system were tested at an angle of 30°, at a flow rate of 8 L/min, the results obtained in the degradation of the organic compound pyridine being sufficient and optimal, using the low ZnO – Ag⁺ doped catalyst—the incidence of sunlight.

The rainwater collected in a cistern was disinfected with the advanced oxidation treatment applied with the RFPD, complying with the NOM-127-SSA1-1994 regulations, considering the principal physical, chemical, and microbiological parameters for water use. It guarantees that this water can be used as drinking water, since the quantitative determination of each parameter was below the maximum permissible limits referenced in the Official Mexican Standard.

Conflict of interest

The authors declare no conflict of interest.

IntechOpen

Author details


Carlos Montalvo^{1*}, Claudia A. Aguilar¹, Rosa A. Martínez¹, Rosa M. Cerón¹,
Alejandro Ruiz¹, Eric Houbbron² and Juan C. Robles¹

1 University Autonomous of Carmen, Carmen City, México

2 University Veracruzana, Veracruz, México

*Address all correspondence to: cmontalvo@pampano.uanacar.mx

IntechOpen

© 2023 The Author(s). Licensee IntechOpen. This chapter is distributed under the terms of the Creative Commons Attribution License (<http://creativecommons.org/licenses/by/3.0>), which permits unrestricted use, distribution, and reproduction in any medium, provided the original work is properly cited. 

References

- [1] Vidales Contreras JA et al. Comportamiento de un sistema de pantanos construidos de flujo superficial para el tratamiento de efluente secundario y de retrolavado. *Tropical and Subtropical Agroecosystems*. 2011;**14**:375-384
- [2] Aurazo, de ZM. Aspectos biológicos de la calidad del agua. In: Tratamiento de agua para consumo humano: Plantas de filtración rápida. Manual I: Teoría. Vol. 1. Lima, Perú. Centro Panamericano de ing. Sanitaria y ciencias ambientales; 2004. pp. 58-102
- [3] Anaya GM. Manual de sistemas de captación y aprovechamiento del agua de lluvia para uso doméstico en América Latina y el Caribe [thesis]. Montecillo, México: IICA, Colegio de Posgraduados; 2004
- [4] CONAGUA. Estadística del agua en México. Síntesis, secretaria de Medio ambiente y recursos Naturales. In Comisión Nacional del Agua. Sistema Nacional de información del Agua. [Internet]. 2022. Available from: https://sina.conagua.gob.mx/publicaciones/Numeragua_2022.pdf [Accessed: June 7, 2023].
- [5] FAO. Captación y almacenamiento de agua de lluvia. Santiago de Chile: FAO; 2013. DOI: 10.1111/jce.13019
- [6] Nava J, Arenas P, Cardoso F. Integrated coastal management in Campeche, Mexico; a review after the Mexican marine and coastal national policy. *Ocean & Coastal Management*. 2018;**154**:34-45. DOI: 10.1016/j.ocecoaman.2017.12.029
- [7] Hassaan MA, El Nemr A. Pesticides pollution: Classifications, human health impact, extraction, and treatment techniques. *The Egyptian Journal of Aquatic Research*. 2020;**46**:207-2020. DOI: 10.1016/j.ejar.2020.08.007
- [8] SEMABICC. Bitácora ambiental. Ordenamiento ecológico territorial del municipio de Carmen. Secretaría de medio ambiente, biodiversidad y cambio climático. Campeche, Mexico; 2013
- [9] Bofill S, Casares P, Giménez N, De Porta C, Gonfa A, Llop R. Efectos sobre la salud de la contaminación de agua y alimentos por virus emergentes humanos. *Revista Española de Salud Pública*. 2005;**79**:253-269. DOI: 10.1590/s1135-57272005000200012
- [10] Allegrini I, Ianniello A, Valentini F. Environmental air pollution: An anthropogenic or a natural issue. In: *Current Trends and Future Developments on (Bio-) Membranes*. Roma Italy: Elsevier; 2023. pp. 1-38. DOI: 10.1016/B978-0-12-824103-5.00007-3
- [11] Rodrigues S, Römkens P. Chapter 9, human health risks and soil pollution. In: *Soil Pollution. Human Health Risks and Soil Pollution*. Portugal: Science Direct; 2018. pp. 217-250. DOI: 10.1016/C2016-0-02243-X
- [12] Babu D, Srivastava V, Nidheesh P, Kumar M. Detoxification of water and wastewater by advanced oxidation processes. *Science of the Total Environment*. 2022;**696**:133961. DOI: 10.1016/j.scitotenv.2019.133961
- [13] Herrmann J. Heterogeneous photocatalysis: Fundamentals and applications to the removal of various types of aqueous pollutants. *Catalysis Today*. 1999;**53**:115-129. DOI: 10.1016/S0920-5861(99)00107-8

- [14] Gisbertz S, Pieber B. Heterogeneous Photocatalysis in organic synthesis. *Chem. Photo. Chem.* 2020;**4**:456-475. DOI: 10.1002/cptc.202000014
- [15] Liu B, Zhao X, Parkin IP, Nakata K. Chapter 4 - charge carrier transfer in photocatalysis. In: *Interface Science and Technology*. Vol. 31. United Kingdom: Elsevier; 2020. DOI: 10.1016/B978-0-08-102890-2.00004-X
- [16] Abdel Messih MF, Ahmed MA, Soltan A, Anis SS. Synthesis, and characterization of novel Ag/ZnO nanoparticles for photocatalytic degradation of methylene blue under UV and solar irradiation. *Journal of Physics and Chemistry of Solids.* 2019;**135**:109086-109104. DOI: 10.1016/j.jpics.2019.109086
- [17] Carbajo J. Aplicación de la fotocatalisis solar a la degradación de contaminantes orgánicos en fase acuosa con catalizadores nanoestructurados de TiO₂ [thesis]. Madrid, Spain: Facultad de Ciencias, Departamento de Química Física Aplicada. Universidad Autónoma de Madrid; 2013
- [18] Malato S, Fernandez P, Maldonado MI, Blanco J, Gernjak W. Decontamination and disinfection of water by solar photocatalysis: Recent overview and trends. *Catalysis Today.* 2009;**147**:1-59
- [19] El-Aassar A, Hameed M, Isawi H, El-Noss M, El-Kholy RA, Said MM, et al. Design and fabrication of continuous flow photoreactor using semiconductor oxides for degradation of organic pollutants. *Journal of Water Process Engineering.* 2019;**32**:100922. DOI: 10.1016/j.jwpe.2019.100922
- [20] Hashim FS, Alkaim AF, Salim SJ, Alkhayatt AHO. Effect of (Ag, Pd) doping on structural, and optical properties of ZnO nanoparticles: As a model of photocatalytic activity for water pollution treatment. *Chemical Physics Letters.* 2019;**737**:136828. DOI: 10.1016/j.cplett.2019.136828
- [21] Lu F, Wang J, Chang Z, Zeng J. Uniform deposition of Ag nanoparticles on ZnO nanorod arrays grown on polyimide/Ag nanofibers by electrospinning, hydrothermal, and photoreduction processes. *Materials and Design.* 2019;**181**:108069. DOI: 10.1016/j.matdes.2019.108069
- [22] Meng X, Zong P, Wang L, Yang F, Hou W, Zhang S, et al. Au-nanoparticle-supported ZnO as highly efficient photocatalyst for H₂O₂ production. *Catalysis Communications.* 2020;**134**:10-13. DOI: 10.1016/j.catcom.2019.105860
- [23] Chong MN, Bo J, Chow CK, Saint C. Recent developments in photocatalytic water treatment technology: A review. *Water Research.* 2010;**44**:2997-3010. DOI: DOI
- [24] Wetchakun K, Wetchakun N, Sakulsermsuk S. An overview of solar/visible light-driven heterogeneous photocatalysis for water purification: TiO₂ and ZnO-based photocatalysts used in suspension photoreactors. *Journal of Industrial and Engineering Chemistry.* 2019;**71**:19-49. DOI: 10.1016/j.jiec.2018.11.025
- [25] Ma W, Li L, Liu Y, Sun Y, Kim I, Ren X. Tailored assembly of vinylbenzyl N-halamine with end-activated ZnO to form hybrid nanoparticles for quick antibacterial response and enhanced UV stability. *Journal of Alloys and Compounds.* 2019;**797**:692-701. DOI: 10.1016/j.jallcom.2019.05.174
- [26] Rosai C, Dilarri G, Froes C, Ruy V, Matos P, Bueno P, et al. Antibacterial action and target mechanisms of

zinc oxide nanoparticles against bacterial pathogens. *Scientific Reports*. 2020;**12**:2658-2670. DOI: 10.1038/s41598-022-06657-y

[27] Alcocer de la HR. Implementación de un sistema de degradación de compuestos orgánicos (piridina) con luz natural y luz uv a diferentes condiciones de operación [thesis]. Campeche: UNACAR Ciudad del Carmen; 2018

[28] NMX-AA-007-SCFI-2013, Water analysis - determination of temperature in natural waters, wastewaters and treated wastewaters – Test method

[29] NMX-AA-008-SCFI-2016, Water analysis-pH measurement in natural, wastewater and treated wastewater" Test method- (CANCELS NMX-AA-008-SCFI-2011)

[30] NMX-AA-034-SCFI-2015. Water analysis - measurement of solids and dissolved salts in natural, wastewater and treated wastewater – Test method (CANCELS NMX-AA-034-SCFI-2001)

[31] NMX-AA-073-SCFI-2001. Water analysis - determination of total chloride in natural, wastewater and treated wastewater - Test method (CANCELS NMX-AA-073-1981)

[32] NMX-AA-072-SCFI-2001. Water analysis - determination of total hardness in natural, residual and treated waste water - Test method (CANCELS NMX-AA072-1981)

[33] NMX-AA-036-SCFI-2001. Water analysis - determination of acidity and alkalinity in natural, wastewater and treated wastewater - Test method (CANCELS NMX-AA-036-1980)

[34] NMX-AA-030-SCFI-2001. Water analysis - determination of the chemical oxygen demand in natural, wastewater

and treated wastewater - Test method (CANCELS NMX-AA-030-1981)

[35] NMX-AA-042-SCFI-2015. Water analysis - enumeration of total coliform organisms, fecal coliform organisms (thermotolerant), and *Escherichia coli* - Most probable number method in multiple tubes (CANCELS NMX-AA-42-1987)

[36] Montalvo C. Degradación fotocatalítica de compuestos que aportan olor al agua residual y potable [thesis]. San Luis Potosí: Universidad Autónoma De San Luis Potosí; 2009

[37] NOM-127-SSA1-1994, “Environmental health, water for human use and consumption-permitted limits of quality and treatments to which the water must be subjected for its potabilization”

[38] Agrawal S, Mandal TK, Mohanty P. Ag⁺ driven antimicrobial activity of Ag⁺: ZnO nanowires immobilized on paper matrices. *Materialia*. 2019;**8**:100490. DOI: 10.1016/j.mtla.2019.100490

[39] Karami A, Xie Z, Zhang J, Kabir MS, Munroe P, Kidd S, et al. Insights into the antimicrobial mechanism of Ag and I incorporated ZnO nanoparticle derivatives under visible light. *Materials Science and Engineering*. 2020;**107**:110220. DOI: 10.1016/j.msec.2019.110220